

INFLUENCE OF THE GALACTIC GRAVITATIONAL FIELD ON THE POSITIONAL ACCURACY OF EXTRAGALACTIC SOURCES

TATIANA I. LARCHENKOVA¹, ALEXANDER A. LUTOVINOV^{2,3}, NATALYA S. LYSKOVA^{4,2}

Draft version August 8, 2018

ABSTRACT

We investigate the influence of random variations of the Galactic gravitational field on the apparent celestial positions of extragalactic sources. The basic statistical characteristics of a stochastic process (first-order moments, an autocorrelation function and a power spectral density) are used to describe a light ray deflection in a gravitational field of randomly moving point masses as a function of the source coordinates. We map a 2D distribution of the standard deviation of the angular shifts in positions of distant sources (including reference sources of the International Celestial Reference Frame) with respect to their true positions. For different Galactic matter distributions the standard deviation of the offset angle can reach several tens of μas (microarcsecond) toward the Galactic center, decreasing down to 4-6 μas at high galactic latitudes. The conditional standard deviation (‘jitter’) of 2.5 μas is reached within 10 years at high galactic latitudes and within a few months toward the inner part of the Galaxy. The photometric microlensing events are not expected to be disturbed by astrometric random variations anywhere except the inner part of the Galaxy as the Einstein–Chvolson times are typically much shorter than the jittering timescale. While a jitter of a single reference source can be up to dozens of μas over some reasonable observational time, using a sample of reference sources would reduce the error in relative astrometry. The obtained results can be used for estimating the physical upper limits on the time-dependent accuracy of astrometric measurements.

Subject headings: Galaxy: general - gravitation - astrometry - reference systems

1. INTRODUCTION

Trigonometric parallaxes, proper motions and angular sizes of celestial bodies, which can be determined only by astrometric methods, are the fundamental quantities in many branches of astronomy and astrophysics. In particular, proper stellar motions and line-of-sight velocities are nowadays the main observational data to investigate the structure of the Galaxy, its gravitational field (the existence of dark matter, the structure of the disk and of the inner bar, the bulge density), and the evolution of the Galaxy (the stability of its spiral structure). The correct handling of astrometric problems requires a reliable celestial reference system, the implementation of which is the coordinate system. A standard reference system in astrometry is the International Celestial Reference Frame (ICRF) constructed by the position measurements of 212 ‘defining’ extragalactic sources (<http://hpiers.obspm.fr/icrs-pc/icrf/catalogues/icrf.def>). These ‘defining’ sources have at least 20 observations with a total duration of at least two years. Quasars and distant galaxies are ideal reference sources for defining the celestial reference system, since their angular motion is ~ 0.01 mas (millisecond of arc) per year (Feissel & Mignard 1998).

In the nearest future, modern technologies will allow us to conduct extremely accurate radio interferometric observations with an angular resolution of 1 μas

and optical observations with an accuracy of 10 μas per year. Analyzing such precise observations, we have to take into account general relativistic effects associated with the propagation of the electromagnetic waves in non-stationary gravitational fields. In this regard, it is important to consider variations in apparent positions (jitter) of extragalactic sources due to the propagation of their emission in the non-stationary gravitational field of both visible stars in the Galactic disk/bulge and invisible massive objects in the halo. Due to its high importance, this topic has been actively investigated since the 1990’s. The astrometric microlensing caused by stars in the Galaxy was discussed, for example, in Dominik & Sahu (2000); Zhdanov & Zhdanova (1995); Sazhin (1996); Yano (2012); Dominik (2006); Dalal & Griest (2001); Lee et al. (2010), and for binary systems in Han et al. (1999); Dominik (1998); Nucita et al. (2016); Sajadian (2015). This is only a short list of the available literature.

It is important to note that any source belonging to the reference coordinate system ICRF is also affected by the jitter of its apparent position. In particular, the improving precision of astrometric observations leads to the fact that the ‘jittering’ of the reference sources can become visible. It is a gravitational noise which does not allow us to increase the accuracy of the implementation of the coordinate system above a certain level. Therefore, there is a natural limitation on the observational accuracy.

Following this discussion, one can say that the measured coordinates of the source can be treated as random functions of time. The time variation of the light deflection from the straight line joining the observer and the source can be considered as a random or stochastic process. This stochastic process can be described by

¹ ASC of P.N.Lebedev Physical Institute, Leninskiy prospect 53, Moscow 119991, Russia;

² Space Research Institute, Russian Academy of Sciences, Profsoyuznaya 84/32, 117997 Moscow, Russia;

³ Moscow Institute of Physics and Technology, Moscow region, Dolgoprudnyi, Russia

⁴ Max-Planck-Institut für Astrophysik, Karl-Schwarzschild-Strasse 1, 85741 Garching, Germany

such statistical quantities as a mathematical expectation, variance, and correlation (autocorrelation) function. The considered characteristics of the stochastic process vary depending on the direction to the source (the closer the line of sight to the Galactic plane, the greater the number of randomly passing stars) and the distance from the source (the further the source, the greater the expected number of passages).

To describe the gravitational noise, we find the basic characteristics (first-order moments, the autocorrelation function, the power spectral density (PSD), and its spectral index) of the light deflection angle in the gravitational field of moving point masses. For this purpose, we follow the method proposed by Larchenkova & Kopeikin (2006). Namely, the deflection angle is considered to be a function of time, i.e. of the impact parameter. In order to calculate the first-order moments, it is necessary to perform the integration over a statistical sample of bodies deflecting the light ray. This statistical sample includes the mass, spatial, and velocity distributions of light-deflecting bodies. Finally, knowing the autocorrelation function of the process allows us to calculate the time-dependent characteristics, such as a conditional variance and a conditional standard deviation. For the small timescales, the conditional variance characterizes the blur of the data for the observation series, while for the large time scales it describes secular variations and tends to the value of the total dispersion. Below, we refer to it as the dispersion, omitting "total".

Note, that this task is quite challenging (as is confirmed by the above-mentioned papers), and we do not pretend here to provide its final and exact solution. Our numerical approach to the problem is based on some simplifying assumptions. The main purposes of this work are the following:

- (1) To calculate basic statistical characteristics, such as the standard deviation of the apparent offset in positions of sources, the autocorrelation function, conditional standard deviations, and the PSD of a stochastic process. This process determined by random passages of Galactic objects close to a line of sight during astrometric observations of distant sources. We perform such calculations for the multicomponent models of the matter distribution in the Galaxy.
- (2) To construct the Galactic map of the conditional and total standard deviations as a visual representation.
- (3) To estimate how the local non-stationary gravitational field of the Galaxy affects the accuracy of measured positions (coordinates) of observed sources including reference sources of the ICRF.

In Section 2, we provide an expression for the light ray deflection angle in the gravitational field of moving massive compact bodies in the Galaxy as well as expressions for the studied characteristics of the stochastic process. Section 3 presents the calculations and describes the method of calculations. All results are briefly discussed in Section 4. The mass, velocity, and spatial distributions of deflecting bodies are given in the Appendices.

2. ANALYTICAL TREATMENT

While propagating through the Galaxy, the light ray from a distant (extragalactic) source experiences multiple events of changing its trajectory due to the presence of a large amount of moving compact massive objects such as stars, stellar remnants, brown dwarfs, etc. The variations of the gravitational field in time created by the Galactic objects (or in other words, the fluctuations of the galactic matter density) can be treated as a stochastic process (e.g., Chandrasekhar 1943).

Obviously, for a stochastic process, it is impossible to predict its instantaneous value. Thus the individual realizations of such a process are described by random functions with values at any given time being random variables. As stated in the Introduction, its main characteristics are the standard deviation, the autocorrelation function, and PSD, the expressions for which can be found, for example, in Pugachev (1960). It is worth mentioning that we assume the Galaxy to be stationary on large scales, while on small scales there are some small variations due to motions of stars and other deflecting compact objects.

Let $\alpha(t, m_a, \vec{X}_a, \vec{v}_a)$ be a function that describes realizations of the random process of the light ray deflection in the Galaxy, where t is time, $\vec{X}_a = (x_a, y_a, z_a)$, m_a, \vec{v}_a are the coordinates, mass and velocity of the a th deflecting body, correspondingly. If the mathematical expectation $\langle \alpha(t) \rangle$ is constant, then the random process is stationary, and the standard deviation can be written as

$$\sqrt{\langle \alpha^2 \rangle} = \sqrt{\int dm_a d\vec{X}_a d\vec{v}_a f(\vec{X}_a, m_a, \vec{v}_a) \alpha^2(\vec{X}_a, m_a, \vec{v}_a)}, \quad (1)$$

where the angular brackets denote averaging over the statistical ensemble, and $f(\vec{X}_a, m_a, \vec{v}_a)$ is the probability density function.

The autocorrelation function $\mathfrak{R}(t_i, t_j)$ of the function $\alpha(t, m_a, \vec{X}_a, \vec{v}_a)$ is

$$\mathfrak{R}(t_i, t_j) = \langle \alpha(t_i, m_a, \vec{X}_a, \vec{v}_a) \cdot \alpha(t_j, m_a, \vec{X}_a, \vec{v}_a) \rangle,$$

where t_i and t_j are different moments in time.

For the stationary random process, the autocorrelation function does not depend on the time instants t_i and t_j , instead, it depends on their difference $\tau = t_i - t_j$, so

$$\begin{aligned} \mathfrak{R}(\tau) &= \langle \alpha(t + \tau) \alpha(t) \rangle = \\ &= \int dm_a d\vec{X}_a d\vec{v}_a f(\vec{X}_a, m_a, \vec{v}_a) \times \\ &\alpha(t, \vec{X}_a, m_a, \vec{v}_a) \alpha(t + \tau, \vec{X}_a, m_a, \vec{v}_a), \end{aligned} \quad (2)$$

where $t = t_j$.

The conditional standard deviation can be written as

$$\sqrt{\langle \alpha^2 | \tau \rangle} = \sqrt{\langle \alpha^2 \rangle (1 - \mathfrak{R}(\tau))}, \quad (3)$$

where $\mathfrak{R}(\tau)$ is a normalized autocorrelation function.

Our calculations show that the mathematical expectation is indeed constant for the large time scales. Thus, the stochastic process, describing variations of the observed extragalactic source position resulting from the impact of moving compact Galactic objects, is expected

to be stationary. Note that it is an expected result since the light ray deflection process is considered in some spatial cone, in which the mean number of incoming particles (stars) is approximately equal to the number of outgoing ones. Based on these arguments, for further calculations, the expressions (1) and (2) are used.

The corresponding PSD can be written as

$$S(\omega) = \frac{1}{2\pi} \int_{-\infty}^{+\infty} \exp(-i\omega\tau) \Re(\tau) d\tau \quad (4)$$

where ω is the frequency of the Fourier decomposition of the autocorrelation function.

Assuming that the statistical ensemble of deflecting bodies is defined by uncorrelated parameters associated with the velocities, masses, and spatial distributions of those deflecting bodies, the probability density can be approximated by a product of three statistically independent probability densities:

$$f(\vec{X}_a, m_a, \vec{v}_a) = Af(\vec{X}_a)f(m_a)f(\vec{v}_a),$$

where the normalization factor A is defined from

$$\int dm_a d\vec{X}_a d\vec{v}_a f(\vec{X}_a, m_a, \vec{v}_a) = 1.$$

We assume here that the integration limits are known and they set the range of variations of the statistical ensemble parameters.

Mass, velocity, and spatial distributions of the deflecting bodies are described in Appendix.

2.1. Deflection angle

In the limit of small deflection angles, the expression for the light ray deflection angle in the gravitational field of a gravitating body was obtained by Einstein. To simplify calculations, we assume that velocities of deflecting bodies are constant in time ($\vec{v}_a = \text{const}$) and a distance between a photon and a deflecting body at a moment of the closest approach is much smaller than any other distances characterizing the system. We use the expression for the deflection of a light ray propagating in the gravitational field of arbitrarily moving massive bodies from Kopeikin & Schäfer (1999):

$$\alpha_a^i(t) = \frac{4Gm_a}{c^2} \frac{1 - \vec{k}\vec{v}_a/c}{\sqrt{1 - v_a^2/c^2}} \frac{P_j^i r_a^j}{|P_j^i r_a^j|^2} \quad (5)$$

where \vec{k} is the unit vector directed from the emitting source to the observer, $|r_a^j|$ is the distance from the a th deflecting body to the observer, c is the speed of light, G is the gravitational constant, $P_{ij} = \delta_{ij} - k_i k_j$ is the operator of projection onto the plane perpendicular to \vec{k} , δ_{ij} is the Kronecker symbol, $i, j = 1, 2, 3$.

Components of the light deflection by the a th body in the Cartesian coordinate system (x, y, z) with the center at the observer position and the Z -axis directed toward the source (see Fig.1) are defined by

$$\alpha_a^x(t) = \frac{4Gm_a}{c^2} \frac{1 - \vec{k}\vec{v}_a/c}{\sqrt{1 - v_a^2/c^2}} \frac{-x_a}{x_a^2 + y_a^2} \left(1 + \frac{z_a}{\sqrt{x_a^2 + y_a^2 + z_a^2}} \right);$$

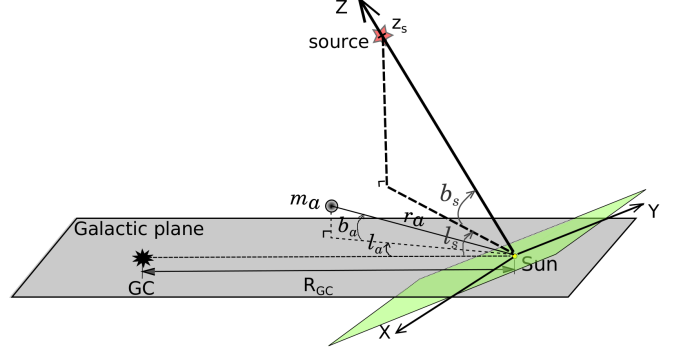


Figure 1. Geometry of the problem. (X, Y, Z) is the Cartesian coordinate system with the Z -axis pointing toward the source. R_{GC} and r_a are the distances from the Sun to the Galactic center and to the a th deflecting body, correspondingly. l_a and b_a are the galactic longitude and latitude of the a th deflecting body, l_s and b_s are the source galactic coordinates.

$$\alpha_a^y(t) = \frac{4Gm_a}{c^2} \frac{1 - \vec{k}\vec{v}_a/c}{\sqrt{1 - v_a^2/c^2}} \frac{-y_a}{x_a^2 + y_a^2} \left(1 + \frac{z_a}{\sqrt{x_a^2 + y_a^2 + z_a^2}} \right); \quad (6)$$

$$\alpha_a^z(t) = 0,$$

and the deflection angle is

$$\alpha_a(t) = \sqrt{(\alpha_a^x(t))^2 + (\alpha_a^y(t))^2} \quad (7)$$

3. RESULTS OF CALCULATIONS

As mentioned above, the main purposes of this paper are the calculation of the autocorrelation function and the creation of the Galactic map of the standard deviation and the conditional standard deviation.

From a mathematical point of view, the calculation of the standard deviation and the autocorrelation function is reduced to the computation of the multi-fold integral over the specified limits of integration

$$\sqrt{\langle \alpha^2 \rangle} = \sqrt{\sum_i \int dm_a d\vec{X}_a d\vec{v}_a f_i(\vec{X}_a) \xi_i(m_a) f_i(\vec{v}_a) \alpha^2(\vec{X}_a, m_a, \vec{v}_a)}, \quad (8)$$

$$\Re(\tau) = \sum_i \int dm_a d\vec{X}_a d\vec{v}_a f_i(\vec{X}_a) \xi_i(m_a) f_i(\vec{v}_a) \times \alpha(t, \vec{X}_a, m_a, \vec{v}_a) \alpha(t + \tau, \vec{X}_a, m_a, \vec{v}_a), \quad (9)$$

where summation is performed over different components of the Galaxy, and $f_i(\vec{X}_a)$, $\xi_i(m_a)$, $f_i(\vec{v}_a)$ are the spatial, mass, and velocity distributions of deflecting bodies (see Appendix). Note, that we use the continuous medium approximation for the complex multicomponent Galactic structure description.

Let us turn to the discussion of the integration limits in the expressions (3) and (9). Integration over masses is

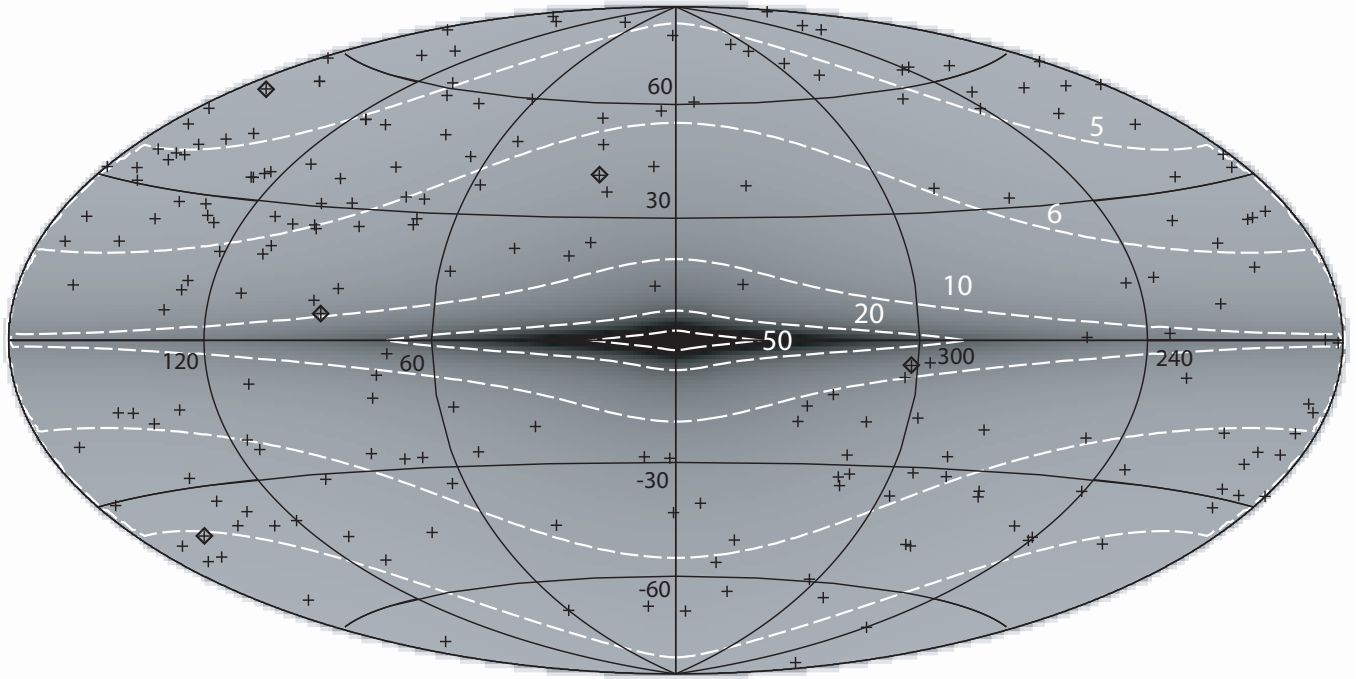


Figure 2. Map of the standard deviation of the angle between the measured and the true source positions on the celestial sphere for the DB model. Dashed lines show contours of the standard deviation $\sqrt{\langle \alpha^2 \rangle}$ in μas . Positions of the ICRF reference sources are marked as crosses. Several reference sources from Table 1 are shown as diamonds.

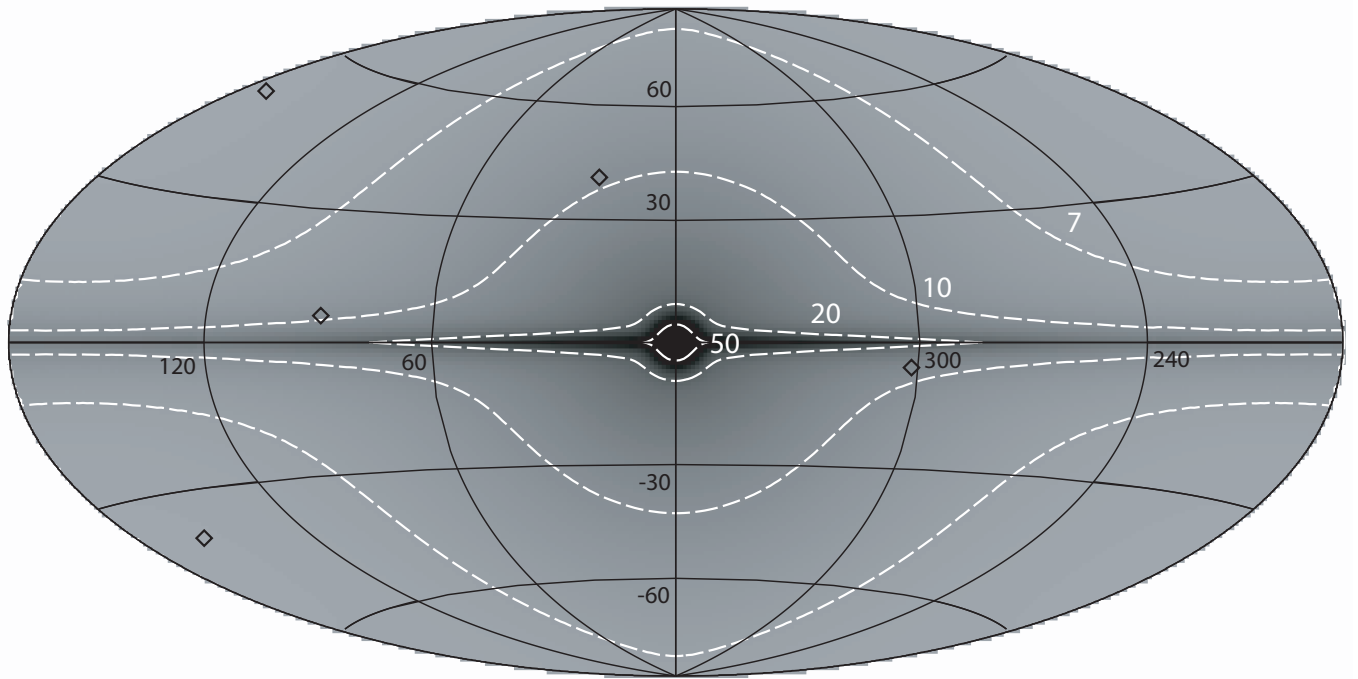


Figure 3. Map of the standard deviation of the angle between the measured and the true source positions on the celestial sphere for the BS model. Dashed lines show contours of the standard deviation $\sqrt{\langle \alpha^2 \rangle}$ in μas . Positions of several reference sources (see Table 1) from the ICRF catalog are marked as diamonds.

done within the limits specified in Appendix A. The integration over the velocity space is performed up to 500 km s^{-1} . When calculating the statistical characteristics of the stochastic process under consideration, we have taken into account the influence of all baryonic galactic matter including its invisible component. The Large and Small Magellanic Clouds have been excluded from the analysis due to their irregular spatial structure, parametrization of which is a nontrivial task. For this reason, the integration over $r_a = \sqrt{x_a^2 + y_a^2 + z_a^2}$ has been done up to 50 kpc.

In this paper, we concentrate on a collective influence of ‘distant’ passages of stars on the apparent position of the observed extragalactic source, i.e. only objects with the impact parameters larger than the Einstein–Chwolson radius⁵ have been taken into account. It is well known that when a star crosses the Einstein–Chwolson cone, the microlensing effect manifests itself in the form of a source brightness amplification and a significant displacement of its apparent position (up to milliarcseconds). Therefore, in our calculations, we have excluded the region with the angular impact parameters smaller than $\sim 3 \times 10^{-9}$ or $\sim 0.6 \text{ mas}$, what approximately corresponds to the Einstein–Chwolson radius for a solar mass star at 20 kpc. The influence of this limitation on the results of calculations will be discussed below.

3.1. Galactic map of the standard deviation

A presence of the supermassive black hole at the Galactic center makes the structure of this area is fairly complex, which cannot be described by a single component. Typically, this area is called ‘the Nuclear Stellar Bulge’ and is believed to be $\sim 30 \text{ pc}$ in size (for more details, see Launhardt et al. 2002). This corresponds to an angle of $\gamma \simeq 0.215^\circ$ assuming the solar Galactocentric distance of 8 kpc. The same value of γ has been taken as a step in coordinates for computing the standard deviation of the angle between the measured and the true positions of the extragalactic source. Taking into account the fact that the density distribution of the matter is given by a smooth function with the characteristic scale of variations significantly exceeding γ , the choice of γ seems to be justified. For the visualization purposes, the obtained results have been converted into a so-called AIT (Aitoff) projection of the celestial sphere in Galactic coordinates and averaged over $1^\circ \times 1^\circ$.

We have calculated the standard deviation $\sqrt{\langle \alpha^2 \rangle}$ for two realistic multicomponent Galaxy models, namely, for the Dehnen & Binney (1998) model (hereafter, DB model) consisting of a three-component disk, a bulge, and a halo, and for the ‘classical’ Bahcall–Soneira model (hereafter, BS model) from (Bahcall & Soneira 1980; Bahcall 1986) which consists of an exponential disk, a bulge, a spheroid, and a halo (for details see Appendix). Figures 2 and 3 present the maps of the standard deviation for the DB and BS models, correspondingly. From these maps, it can be seen that the increase of the standard deviation is expected in the direction to the Galactic center and the Galactic plane as the matter density increases. In particular, in the direction to the Galac-

Table 1

The standard deviation $\sqrt{\langle \alpha^2 \rangle}$ (in μas) of the angle between the measured and the true position for several ICRF reference sources computed for different models of the matter density distribution in the Galaxy.

Source Name	l°, b°	$\sqrt{\langle \alpha^2 \rangle}$, DB	$\sqrt{\langle \alpha^2 \rangle}$, BS
J023838.9+163659	156.7, -39.1	4.8	5.8
J095819.6+472507	170.0, 50.7	4.6	5.8
J123946.6-684530	301.9, -5.9	11.4	10.9
J160846.2+102907	23.0, 40.8	6.5	9.3
J203837.0+511912	88.8, 6.0	9.3	9.2

tic center the standard deviation of the deflection angle reaches several tens of microarcseconds, exceeding $50 \mu\text{as}$ in the central region with the size of $\sim 6^\circ \times 2^\circ$ for the DB model, and decreasing down to 4-6 μas at the high galactic latitudes. The obtained maps reflect in general the matter distribution in the Galaxy represented by different models. In particular, the map for the BS model is characterized by more spherical contour lines than the map for the DB model, which is caused by the spherical bulge and the stellar spheroid in the BS model.

Positions of 212 reference extragalactic sources of the ICRF (<http://hpiers.obspm.fr/icrs-pc/icrf/catalogues/icrf.def>) are shown also in Fig. 2. With increasing an absolute accuracy of space-based astrometric measurements, it will become necessary to take into account the discussed jitter of reference sources coordinates caused by the local non-stationary Galactic gravitational field. Moreover, for about a dozen of reference sources in the Galactic plane, the standard deviation of the deflection angle can reach $> 10 \mu\text{as}$. For a visual comparison of the standard deviations calculated for DB and BS models, we present the standard deviation values for several reference sources in Table 1. The positions of these sources are marked in Fig. 2 and 3 as diamonds; two sources out of five are located in the Galactic plane (at low galactic latitudes), and three others at high latitudes. As seen from Table 1 the values of the standard deviations for both models of the Galaxy are close to each other.

As mentioned above, to exclude photometric microlensing events from consideration, we have introduced the lower limit of integration over coordinates (i.e., the minimal impact parameter) and have set its value to 3×10^{-9} . We have investigated how obtained results are sensitive to a particular choice of the this parameter. One order of magnitude variation of the minimal impact parameter from 2×10^{-9} (this value approximately corresponds to the Einstein–Chwolson radius R_{EC} for a solar mass star at a distance of 50 kpc from the observer) to 1.4×10^{-8} (corresponds to $\simeq R_{EC}$ for a solar mass star at 1 kpc) has introduced only $\simeq 10\%$ variations in the standard deviation. A further increase of this lower limit up to 2×10^{-7} (corresponds to $\simeq R_{EC}$ for a solar mass star at 5 pc) lowers the standard deviation value by about 20%. Note, that the latter value of the lower limit of integration clearly exceeds the Einstein–Chwolson radii for the stars in the Galaxy. Thus, we conclude that the calculated value of the standard deviation is rather stable against sufficient variations of the minimal impact

⁵ The Einstein–Chwolson radius is the radius of a ring-like image of the background source, which appears when the observer, the lens, and the source are precisely aligned.

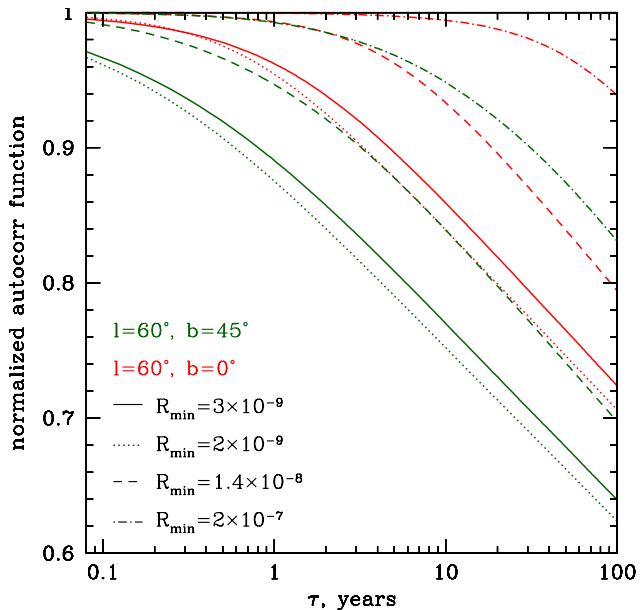


Figure 4. Normalized autocorrelation functions calculated for the DB model for two directions in the sky at different minimal impact parameters.

parameter.

It is important to note that the maps in Figures 2 and 3 give an order of magnitude estimate of the standard deviation of the distribution of deflection angles. For practical applications, we still need to know typical values of the variations, which can be revealed at reasonable time scales of observations. Corresponding time-dependent statistical characteristics will be discussed in the next sections.

3.2. Autocorrelation function, PSD and conditional standard deviation

Useful tools for describing stationary processes are an autocorrelation function and a corresponding PSD, each of which characterizes different properties of observational data. Therefore, as a first step, we have computed the autocorrelation function (Eq.9) on time scales of up to 100 years for different directions on the celestial sphere. These autocorrelation functions can be formally approximated by a superposition of several components decreasing exponentially with different characteristic times T_i .

In contrast to the standard deviation, the characteristic decay time of exponents depends not only on the direction on the celestial sphere but also on the lower limit of integration over coordinates (R_{\min}) what can be seen from Fig.4. Note, that the behavior of autocorrelation functions for both galactic models (DB and BS) is similar; therefore, in the following analysis, we are restricted only by the DB model. With increasing of R_{\min} , i.e. with increasing the minimal impact parameter, the characteristic decay time of exponents becomes larger, which seems quite natural. At the same time, varying the parameters of calculation does not affect an exponential form of the normalized autocorrelation function.

For the autocorrelation function in a form of a decaying

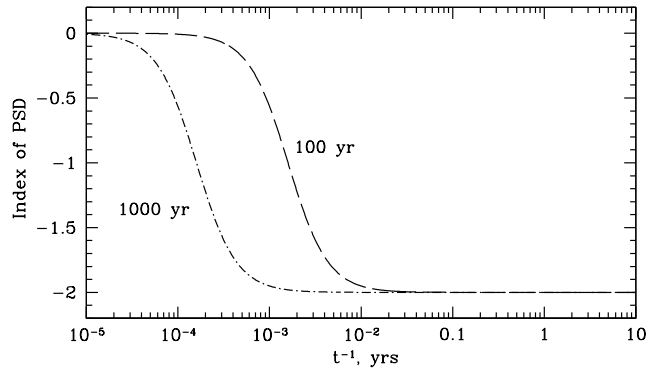


Figure 5. Spectral index of PSD calculated for two exponents with the characteristic time of 100 and 1000 days.

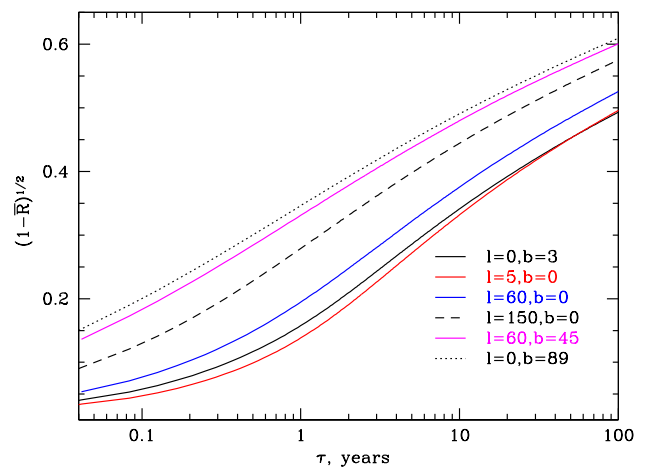


Figure 6. Coefficient $\sqrt{1 - \mathfrak{R}}$ calculated for the DB model for different directions in the sky with $R_{\min} = 3 \times 10^{-9}$.

exponent $e^{-\tau/T}$ the PSD is simply

$$PSD \propto \frac{T^2}{1 + 4\pi^2 T^2 \omega^2}, \quad (10)$$

where T is characteristic time of the exponent, and $\omega = \tau^{-1}$. From this formula and Fig. 5 it is clearly seen that on the reasonable observing time-scales (up to one hundred years) the PSD index equals to -2 for any direction on the celestial sphere and does not depend on the characteristic time. Thus, if an analysis of the apparent celestial positions of extragalactic sources, including the reference sources of the ICRF, reveals a component with a slope of -2 in their power spectra, this component can be explained by the collective influence of stars and compact objects in the Galaxy.

For the analysis of astrometric observations of staggering precision, it is important to know an expected value of the jitter of reference sources, arising due to the local non-stationarity of the Galactic gravitational field, for a specific time interval. Intuitively, the larger the time interval between observations, the greater the relative offset of sources can be. If we know the behavior of the autocorrelation function of the studied process in time, we can predict the expected value of the jitter (dispersion) for any time interval. For illustration purposes,

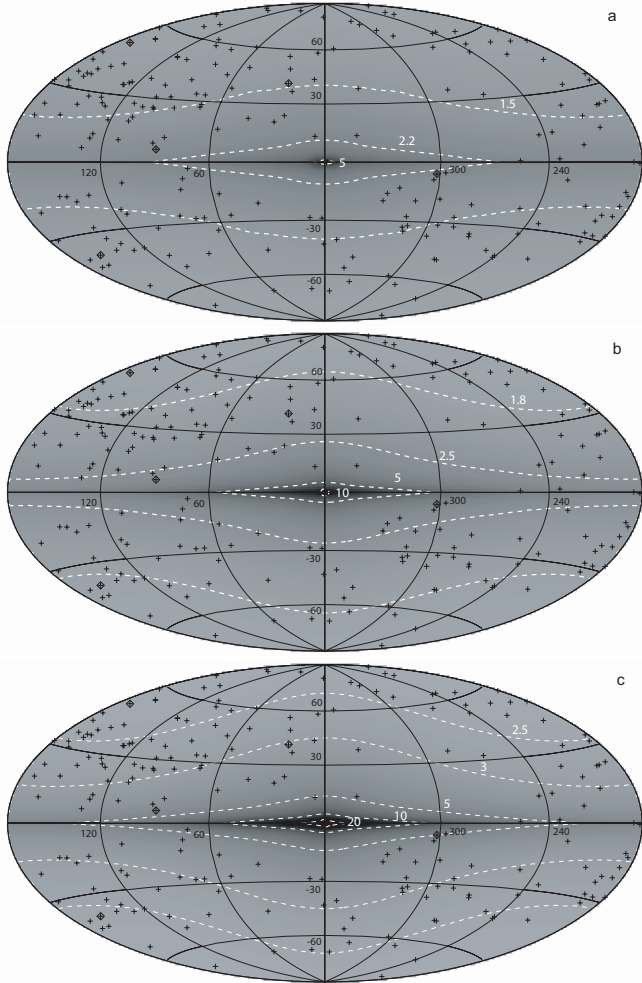


Figure 7. Map of the conditional standard deviation of the angle between the measured and the true source positions on the celestial sphere for the DB model for different observational intervals: 3 months (a), 1 year (b), 10 years (c). Dashed lines show contours of the conditional standard deviation in μas .

the dependence of the coefficient $\sqrt{1 - \mathfrak{R}}$ (Eq. 3) on time is shown in Fig. 6. This coefficient has been calculated for the DB model for different directions in the sky, and for $R_{\min} = 3 \times 10^{-9}$. To obtain maps of the conditional standard deviation (see Eq. 3) the corresponding coefficients were determined for all sky directions for three time intervals (three months, one year, and ten years) and convolved with the dispersion map (Fig. 2). The resulting maps of the conditional standard deviation are presented in Fig. 7. From these maps, it is clearly seen that the jitter may reach a few and a dozen of μas in the direction toward the central parts of the Galaxy at the time scales of 1 and 10 years, respectively, decreasing down to $1 \mu\text{as}$ at high galactic latitudes.

4. DISCUSSION AND CONCLUSION

In this paper, we have examined the impact of the random variations of the Galactic gravitational field on the apparent celestial position of extragalactic sources. The influence of all galactic baryonic matter including the invisible (non-luminous) components such as brown dwarfs has been taken into account. The Large and Small Magellanic Clouds were excluded from consideration due to

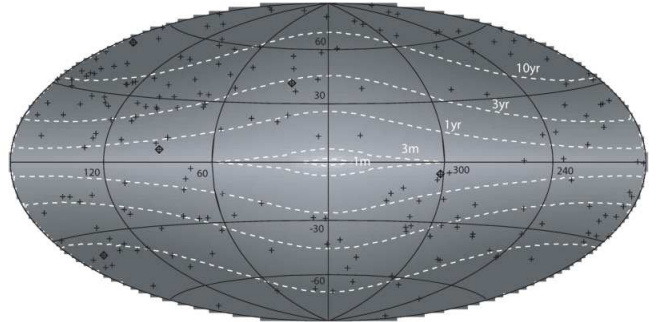


Figure 8. Map of the jitter time-scale at $\delta_T = 2.5 \mu\text{as}$. Dashed lines show contours in months and years.

Table 2

The estimated jitter time (in years) at $\delta_T = 2.5 \mu\text{as}$ for several ICRF reference sources.

Source Name	l°, b°	$t_{jit, 2.5 \mu\text{as}}, \text{yrs}$
J023838.9+163659	156.7, -39.1	> 10
J095819.6+472507	170.0, 50.7	> 10
J123946.6-684530	301.9, -5.9	0.4
J160846.2+102907	23.0, 40.8	2.6
J203837.0+511912	88.8, 6.0	0.6

their complex irregular spatial structure, which is hard to parameterize. We have obtained the basic statistical characteristics (mathematical expectation, standard deviation, autocorrelation function, PSD, and its spectral index) of a stochastic process describing variations of the extragalactic source positions (coordinates) on the celestial sphere caused by the deflection of light rays in the gravitational field of randomly moving point masses. We have mapped the two-dimensional distribution of the standard deviation of the deflection angle between the measured and the true positions of distant sources including the reference sources of the ICRF (Figs. 2, 3). These maps give the order of magnitude of the expected value of the standard deviation. For these models of the matter density distribution, it has been shown that in the direction towards the Galactic center the standard deviation of the deflection angle (jitter) can reach several tens of μas , exceeding $50 \mu\text{as}$ in the very central region (with the size of $\sim 6^\circ \times 2^\circ$) and decreasing down to $4 - 6 \mu\text{as}$ at high galactic latitudes.

This jitter effect imposes principal limitations on improving the accuracy of absolute astrometric measurements, making problematic the further improvement of observation precision due to the emerging ‘gravitational’ noise. Nevertheless, based on the theoretical estimates of statistical characteristics of this noise, it is possible to identify it in the analysis of observational data. The knowledge of the autocorrelation function allow us to calculate the PSD and the corresponding spectral index of the ‘gravitational’ noise generated by random passages of Galactic objects close to the line of sight. It has been shown that the obtained autocorrelation functions can be formally approximated by a superposition of several components decaying exponentially with different characteristic times. For observing time scales up to 100 years the spectral index of the PSD equals to -2 for any direction

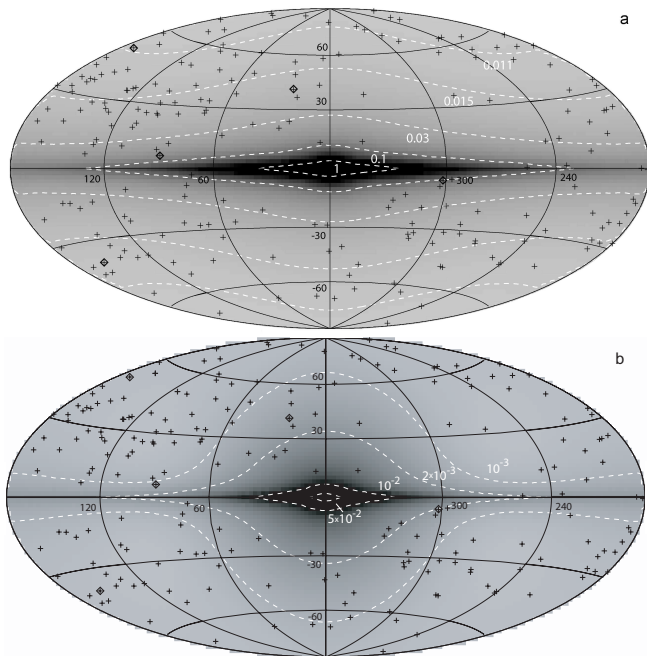


Figure 9. Maps of the astrometric microlensing optical depth (a) and the astrometric event rate (b) for the DB model for the threshold $\delta_T = 2.5 \mu\text{as}$. Dashed lines show contours of the astrometric microlensing optical depth (a) and the astrometric event rate in yr^{-1} (b).

on the celestial sphere and does not depend on (internal) parameters of integration. Thus, if the analysis of apparent celestial positions of extragalactic sources, including the reference sources of the ICRF, reveals a component with a slope of -2 in its power spectrum, this component can be explained by the collective influence of stars and compact objects in the Galaxy and, in principle, can be extracted.

In practice, it is important to know an expected value of the jitter of reference sources, arising from the local non-stationarity of the Galactic gravitational field, for a specific time interval. The autocorrelation function of the studied process allow us to predict the expected value of the jitter (the conditional standard deviation) for any time interval. We have constructed corresponding maps for three observational time intervals (3 months, 1 and 10 years) and showed that the jitter may reach about a few and a dozen of μas in the direction toward the central parts of the Galaxy at the time scales of 1 and 10 years, respectively, decreasing down to $\simeq 1 \mu\text{as}$ at high galactic latitudes (Fig. 7).

Additionally, for planning and performing astrometric observations it would be important to estimate the jitter time in which the local variations of the Galactic gravitational field will produce an astrometric signature larger than or equal to a given astrometric precision δ_T . This time can be estimated from the autocorrelation function by the inverse solution of Eq. 3. As an example, we have constructed the map of the expected jitter times for the astrometric accuracy of $\delta_T = 2.5 \mu\text{as}$ (Fig. 8). From this map, it is seen that such the jitter can be produced by random variations of the gravitational field of the Galaxy at time-scales of 3-10 years at high galactic latitudes ($> 30^\circ$) and at time-scales of only several months in the inner part of the Galaxy. The jit-

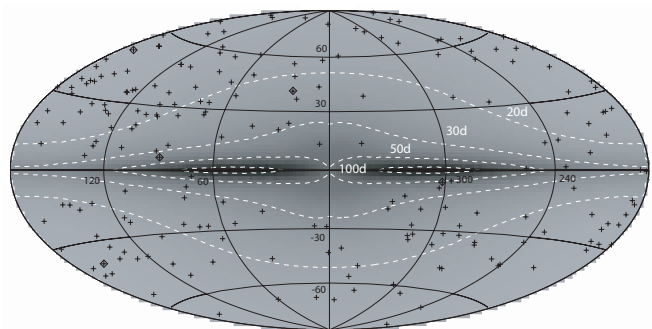


Figure 10. Map of the Einstein–Chwolson crossing time $\langle t_E \rangle$. Dashed lines show contours in days.

ter time estimated for $\delta_T = 2.5 \mu\text{as}$ for several reference sources (the same ones as in Table 1) are listed in Table 2 for illustrative purposes. The jitter times for other values of the astrometric accuracy δ_T can be preliminarily estimated from Fig. 2 and autocorrelation functions (Fig. 6).

It is obvious that if the jitter time-scale results are much larger than the observational time, then the reference sources are ‘fixed’ in space, and can be used as references for any purpose. If this is not the case, the associated errors used in reconstructing the astrometry should be taking into account. At the same time, it is necessary to note that while the jitter of a single reference source can be up to dozens of μas over some reasonable observational time, using a sample of reference sources would greatly reduce the error in relative astrometry.

We have also calculated the maps of the astrometric microlensing optical depth and the event rate of extragalactic sources for the detection threshold $\delta_T = 2.5 \mu\text{as}$. It is important to note that these values for the microlensing of distant sources are significantly different from ones for the microlensing of stars in the Galaxy. In particular, Honma & Kurayama (2002) demonstrated that the optical depth of astrometric microlensing caused by disk stars for extragalactic source is larger by an order of magnitude than that for stars of the Galaxy. Our calculations show that for extragalactic sources the astrometric optical depth reaches 1 (i.e., the probability that a source position shift exceeds a given threshold $2.5 \mu\text{as}$ is 100%) and the event rate is $\sim 0.05 \text{ events yr}^{-1}$ in the central parts of the Galaxy. Both values decrease by two orders of magnitude at high galactic latitudes (Fig. 9). These estimations are generally agreed with results of calculations performed by other authors under their assumptions (see, e.g., Honma & Kurayama 2002; Dominik & Sahu 2000; Evans & Belokurov 2002). The average duration of the astrometric event can be estimated from corresponding values of the optical depth and the event rate (see, e.g., Dominik & Sahu 2000).

Another possibly interesting and important question is whether the jitter has an impact on the observational properties of sources, in particular, on the registration of photometric microlensing events. To answer this question, we have calculated the map of the Einstein–Chwolson crossing time $\langle t_E \rangle$, which is the time taken for the source to cross the Einstein–Chwolson radius (Fig. 10). A comparison of this map with the time jitter map (Fig. 8) shows that photometric microlensing events are not expected to be disturbed by the astromet-

ric random variations anywhere except the inner part of the Galaxy, as the Einstein–Chvolson times are typically much shorter than the jittering time-scale for the detection threshold of $\delta_T = 2.5\mu\text{as}$.

Summarizing all above, we can conclude that the obtained results can be used for estimations of the physical upper limits on the time-dependent accuracy of astrometric measurements. Therefore, as soon as space-based observations reach an absolute astrometric accuracy of microseconds of arc, it will be necessary to take into account the ‘jitter’ of reference source coordinates caused by the local non-stationary gravitational field of Galaxy.

5. ACKNOWLEDGMENTS

This work was supported by the Russian Science Foundation (grant 14-22-00271). T.L. acknowledges a partial support by the program of the Presidium of RAS (P-7) and the Grant of the President of the Russian Federation for Support of the Leading Scientific Schools NSh-6595.2016.2. We thank Artur Matveev for his help with numerical calculations and A.Doroshkevich and D.Novikov for a careful reading of the manuscript and discussing results. We thank the anonymous referee for useful comments and suggestions that certainly improved the manuscript.

APPENDIX

A. MASS DISTRIBUTION OF DEFLECTING BODIES

The number of stars (and brown dwarfs) per unit mass is the stellar mass function (MF), which is usually given in linear units (stars $pc^{-3}M_\odot^{-1}$) or in logarithmic units (stars $pc^{-3}\log^{-1}(M_\odot)$). It is important to note that there is no direct observational determination of the MF. What is observed is the individual or integrated light of objects, i.e. the luminosity function or the surface brightness. Transformation of this observable quantity into the MF thus relies on theories of stellar evolution (mass–age–luminosity relations). All stars with main-sequence lifetimes greater than the age of the Galaxy are still on the main sequence (Miller & Scalo 1997). In that case, the present-day mass function (PDMF) and the initial mass function (IMF) are equivalent, in particular, the PDMF and the IMF of the low-mass part of MF ($m \leq 1M_\odot$) are equivalent (see, e.g., Chabrier 2003).

The PDMFs for stars (including brown dwarfs) of the Galactic disk, bulge, spheroid, and halo were taken from Chabrier & Mera (1997); Zoccali et al. (2000); Chabrier (2003) as follows:

$$\xi_a(\log m) = \frac{1}{\log M_\odot pc^3} \times \begin{cases} 0.158m^0, & 0.01 \leq m < 0.08 \\ 0.158 \exp \left[-\frac{(\log(\frac{m}{0.079}))^2}{0.9577} \right], & 0.08 \leq m < 1.0 \\ 0.044m^{-4.37}, & 1.0 \leq m < 3.47 \\ 0.015m^{-3.53}, & 3.47 \leq m < 18.2 \\ 2.5 \times 10^{-4}m^{-2.11}, & 18.2 \leq m < 63 \end{cases} \quad (\text{A1})$$

for the disk;

$$\xi_h(m) = 4 \times 10^{-3} \left(\frac{m}{0.1M_\odot} \right)^{-1.7} \frac{1}{M_\odot pc^3}, \quad 0.01 \leq m < 0.8; \quad (\text{A2})$$

for the halo;

$$\xi_{sph}(\log m) = \frac{1}{\log M_\odot pc^3} \times \begin{cases} 3.6 \times 10^{-4} \exp \left[-\frac{(\log(\frac{m}{0.22}))^2}{2(0.33)^2} \right], & m \leq 0.7 \\ 7.1 \times 10^{-5}m^{-1.3}, & m > 0.7. \end{cases} \quad (\text{A3})$$

for the spheroid. For the bulge, we used an expression (A1), but only for $m < 1M_\odot$. Here, M_\odot is the mass of the Sun and m is mass of the star in solar mass units.

The total matter density in the solar vicinity

$$\rho_{total,solar} = \sum_i \int_{m_{min}}^{m_{max}} M \xi_i(M) dM, \quad i = d, b, sph, h$$

is determined in frames of considered models of the Galaxy (see Appendix C), where m_{min} and m_{max} are the minimal and maximal masses for each of the galactic components. Note, that the local dynamical density derived from Hipparcos data is about $0.122M_\odot pc^{-3}$ (van Leeuwen 2007).

B. VELOCITY DISTRIBUTION OF DEFLECTING BODIES

For the velocity distribution of deflecting bodies, we adopt the Maxwell distribution with a cut-off at some v_e :

$$f_i(v_a) = A_v \frac{\exp\left(-\frac{v_a^2}{\sigma_i^2}\right) - \exp\left(-\frac{v_e^2}{\sigma_i^2}\right)}{1 - \exp\left(-\frac{v_e^2}{\sigma_i^2}\right)}, \quad (\text{B1})$$

where A_v is a normalization factor and σ_i is a characteristic stellar velocity dispersion. In general, its value is different for different components of the Galaxy; therefore, in following calculations, we used $\sigma \simeq 100 \text{ km s}^{-1}$ for the halo and spheroid (Xue et al. 2008) and $\sigma \simeq 30 \text{ km s}^{-1}$ for the disk and bulge (see, e.g., Chen 1998; Alcobe & Cubarsi 2005). The quantity v_e plays a role of the second cosmic speed, i.e. the minimal speed at which a star is able to escape the local gravitational field of the Galaxy. According to Carney & Latham (1987); Smith et al. (2007) $v_e \simeq 500 \text{ km s}^{-1}$.

C. SPATIAL DISTRIBUTION OF DEFLECTING BODIES

Because we concentrate here only on the stationary part of the light ray deflection process caused by the varying in time Galactic gravitational field. We exclude from consideration the non-stationary part of the effect, i.e. the influence of individual deflecting bodies crossing the line of sight, which manifests itself as short-term bursts.

As a plausible model of the spatial distribution of deflecting bodies in the Galaxy, we use the multicomponent model of the Galaxy from Dehnen & Binney (1998) (hereafter, DB model) consisting of a three-component disk, a bulge, and a halo. The distribution of the matter density in the cylindrical coordinates (R, z) centered at the Galactic center for each of the three components of the disk is given by

$$\rho_d^{DB}(R, z) = \frac{\sum_d}{2z_d} \exp\left(-\frac{R_m}{R} - \frac{R}{R_d} - \frac{|z|}{z_d}\right), \quad (\text{C1})$$

where R_d and z_d are the characteristic length and height of the disk correspondingly, \sum_d is the central surface density of the disk, and R_m is a parameter describing the decrease in the central surface density of the interstellar medium. R_m is equal to 0 for the thin and thick stellar disks and equals 4 kpc for the disk of the interstellar medium (interstellar gas).

We exclude the interstellar medium disk from consideration since only the deflection by compact objects is of interest to us. According to the model 2 from Dehnen & Binney (1998) the total mass of the disk is $4.88 \times 10^{10} M_\odot$, and $R_d = 2.4$ kpc, $z_d = 180$ pc for the thin disk, and $z_d = 1$ kpc for the thick disk.

The bulge and halo density distributions in the framework of this model are

$$\rho_b^{DB}(R, z) = \rho_{0,b} \left(\frac{\sqrt{R^2 + z^2/q_b^2}}{R_{0,b}}\right)^{-1.8} \exp\left(-\frac{R^2 + z^2/q_b^2}{R_{t,b}^2}\right) \quad (\text{C2})$$

$$\rho_h^{DB}(R, z) = \rho_{0,h} \left(1 + \frac{\sqrt{R^2 + z^2/q_h^2}}{R_{0,h}}\right)^{-4.207} \left(\frac{R^2 + z^2/q_h^2}{R_{0,h}^2}\right), \quad (\text{C3})$$

where the central bulge density is $\rho_{0,b} = 0.7561 M_\odot/\text{pc}^3$, the characteristic bulge radius is $R_{0,b} = 1$ kpc, the truncation radius of the bulge is $R_{t,b} = 1.9$ kpc, the bulge ellipticity is $q_b = 0.6$, the central halo density is $\rho_{0,h} = 1.263 M_\odot/\text{pc}^3$, $R_{0,h} = 1.09$ kpc, and the halo ellipticity is $q_h = 0.8$.

The matter density in the vicinity of the Sun $\rho_{total,solar}^{DB} \simeq 0.083 M_\odot/\text{pc}^3$ for the model under consideration, and the solar Galactocentric distance is $R_{GC} = 8$ kpc.

The spatial distribution function of compact galactic sources in the DB model can be written as follows.

$$f_i(R, z) = \frac{\rho_i^{DB}(R, z)}{\rho_{total,solar}^{DB}}, \quad i = d, b, h \quad (\text{C4})$$

For comparison, we also use another model of the Galaxy density distribution – the ‘classical’ Bahcall-Soneira model (hereafter, BS model) from Bahcall & Soneira (1980); Bahcall (1986), which consists of an exponential disk, a bulge, a spheroid, and a halo. The corresponding density distributions for the galactic components are given by

$$\rho_d^{BS}(R, z) = \rho_{\odot,d}^{BS} \exp\left(\frac{R_{GC} - R}{3.5 \text{ kpc}} - \frac{|z|}{0.125 \text{ kpc}}\right), \quad (\text{C5})$$

$$\rho_b^{BS}(R, z) = \rho_{0,b}^{BS} \left(\frac{\sqrt{R^2 + z^2}}{1 \text{ kpc}}\right)^{-1.8} \exp\left[-\left(\frac{\sqrt{R^2 + z^2}}{1 \text{ kpc}}\right)^3\right] \quad (\text{C6})$$

$$\rho_{sph}^{BS}(R, z) = \rho_{0,sph}^{BS} \frac{\exp\left[-b\left(\frac{\sqrt{R^2 + z^2}}{2.8 \text{ kpc}}\right)^{1/4}\right]}{\left(\frac{\sqrt{R^2 + z^2}}{2.8 \text{ kpc}}\right)^{7/8}} \quad (\text{C7})$$

$$\rho_h^{BS}(R, z) = \rho_{\odot, h}^{BS} \frac{a^2 + R_{GC}^2}{a^2 + R^2 + z^2}, \quad (C8)$$

where the central bulge density is $\rho_{0, b}^{BS} = 1.43 \text{ M}_{\odot}/\text{pc}^3$, the central spheroid density is $\rho_{0, sph}^{BS} = 1/500 \rho_{0, d}^{BS} \simeq 0.00079 \text{ M}_{\odot}/\text{pc}^3$, the disk density in the vicinity of the Sun is $\rho_{\odot, d}^{BS} = 0.04 \text{ M}_{\odot}/\text{pc}^3$, the halo density in the vicinity of the Sun is $\rho_{\odot, h}^{BS} = 0.01 \text{ M}_{\odot}/\text{pc}^3$, and $b = 7.669$. The core radius of halo a is believed to lie in the range from ≈ 2 to 8 kpc. We assume in our estimation that $a = 2$ kpc.

The spatial distribution function of compact galactic sources in the BS model is as follows.

$$f_i(R, z) = \frac{\rho_i^{BS}(R, z)}{\rho_{total, solar}^{BS}}, \quad i = d, b, sph, h \quad (C9)$$

For the BS model $\rho_{total, solar}^{BS} \simeq 0.05 \text{ M}_{\odot}/\text{pc}^3$ (Bahcall & Soneira 1980).

REFERENCES

- Alcobe S., Cubarsi R. 2005, A&A, 442, 929
Bahcall J., Soneira R. M. 1980, ApJS, 44, 73
Bahcall J. 1986, ARA&A, 24, 577
Carney B. W., Latham D. W. 1987, Proceedings of the IAU Symposium, 39
Chabrier G. 2003, PASP, 115, 763
Chabrier G., Mera D. 1997, A&A, 328, 83
Chandrasekhar S. 1943, Rev.Mod.Phys, 15, 1
Chen B. 1998, ApJ, 495, L1
Dalal N., Griest K. 2001, ApJ, 561, 481
Dehnen W., Binney J. 1998, MNRAS, 294, 429
Dominik M. 2006, MNRAS, 367, 669
Dominik M. 1998, A&A, 333, 893
Dominik M., Sahu K. C. 2000, ApJ, 534, 213
Evans, N. W., & Belokurov, V. 2002, ApJ, 567, L119
Feissel M., Mignard F. 1998, A&A, 331, 33
Griest, K. 1991, ApJ, 366, 412
Han C., Chun M., Chang K. 1999, ApJ, 526, 405
Honma M., Kurayama T. 2002, ApJ, 568, 717
Kopeikin S. M., Schäfer G. 1999, PhRvD, 60, 124002
Larchenkova T. I., Kopeikin S. M. 2006, AstL, 32, 18
Launhardt R., Zylka R., Mezger P. G. 2002, A&A, 384, 112
Lee C. H., Seitz S., Riffeser A., Bemder R. 2010, MNRAS, 407, 1597L
Miller G., Scalo J. 1979, ApJS, 41, 513
Nucita A. A., De Paolis F., Ingrosso G., Giordano M., Manni L. 2016, ApJ, 823, 120
Pugachev V. S. 1960, The theory of stochastic functions, Moscow
Sajadian S. 2015, AJ, 149, 147
Sazhin M. V. 1996, AstL, 22, 573
Schneider P., Ehlers J., Falco E.E. 1999, Gravitational Lenses, Berlin, Springer
Smith M. C., Ruchti G. R., Helmi A. et al. 2007, MNRAS, 379, 755
Xue X. X., Rix H. W., Zhao G. et al. 2008, ApJ, 684, 1143
Yano T. 2012, ApJ, 757, 189
Zhdanov V. I., Zhdanova V. V. 1995, A&A, 299, 321
Zoccali M., Cassisi S., Frogel J. A. et al. 2000, ApJ, 530, 418
van Leeuwen F. 2007, Hipparcos, the New Reduction of the Raw Data, Astrophysics and Space Science Library, Vol. 350, Berlin: Springer